

## Orbital Physics in $f$ -Electron Systems

Andrea Severing<sup>#</sup>, Andrea Marino, Martin Sundermann, Denise Sacramento Christovam, Peter Thalmeier and Liu Hao Tjeng<sup>##</sup>

**The group investigates the electronic structure of  $f$ -electron materials, with a particular focus on Ce- and U-based intermetallic compounds, utilizing state-of-the-art x-ray spectroscopy. While addressing ongoing questions in the field of strongly correlated  $f$ -electron science, the group places special emphasis on developing new experimental and analytical techniques to better understand intermetallic uranium compounds, where inconsistent results in the literature have caused growing frustration within the scientific community.**

Among  $f$ -electron materials, particularly those containing Ce and U compounds, a plethora of exciting phenomena have been observed. These include heavy fermion behavior [1,2], hidden order, unconventional magnetism, unconventional superconductivity, the coexistence of ferromagnetism and superconductivity [3–5], orbital multicomponent phenomena [6], and spin-triplet superconductivity [7–9] with unusual topological properties [10]. The hybridization of  $f$  and conduction electrons drives these intriguing low-temperature properties, making the understanding of  $f$ -electronic structures indispensable. Notable newcomers to this exciting field of research include CeRh<sub>2</sub>As<sub>2</sub>, a new multiphase superconductor [11], and UTe<sub>2</sub>, a spin-triplet superconductor candidate [7].

In rare earth elements, with their spatially well-localized  $4f$  electrons, and in transition metals, with their spatially extended  $d$ -electrons, there is a clear hierarchy of interactions, including Coulomb repulsion, spin-orbit coupling, hopping, and crystal-field effects. However, this hierarchy is lost in the actinide series because the  $5f$  electrons lie in-between. Consequently, it becomes challenging to quantitatively describe the electronic structure of  $5f$  intermetallics. It remains unclear whether an itinerant band approach or an impurity-type model, which explicitly accounts for local degrees of freedom, is more suitable.

This complexity is further compounded by the lack of crucial information, such as the formal valence, the actual filling of the  $5f$  shell, the degree of covalence, and the relevant symmetries of the  $5f$  electrons. For instance, determining the formal valence of U compounds is difficult because x-ray absorption spectra (XAS) are very broad (approximately 8 eV at the U  $M_{4,5}$  edge), obscuring potential multiplet structures beneath them [12]. Similarly, core-level photoelectron spectroscopy (PES) spectra typically exhibit a single broad main emission line, with at most one satellite feature [13, 14]. Interpreting such data is challenging, often leading to conflicting interpretations of x-ray data for U intermetallics.

Therefore, while the study of topical Ce compounds using well-established x-ray methods continues [15–20], the group's recent efforts have shifted towards devel-

oping new experimental techniques and approaches to better describe the electronic structure of U intermetallic compounds [21–24].

Element-specific Inelastic X-ray Scattering (IXS), including both resonant (RIXS) and non-resonant (NIXS) techniques, serves as an important and innovative tool. Using NIXS at large momentum transfers at the U  $O_{4,5}$  edges ( $5d \rightarrow 5f$ ), the group demonstrated that, unlike the dipole signal in XAS, the multipole signal is excitonic and can be modeled with an ionic calculation [25,26] using the *QUANTY* code by M.W. Haverkort [27]. Even the dichroism can be described within a local crystal-field model, confirming the presence of multiplets.

However, measuring  $ff$  excitations directly with RIXS in U intermetallics is challenging compared to Ce, because the RIXS signal at the U  $O_{4,5}$  edges ( $5d \rightarrow 5f$ ) lies in the extreme ultraviolet and is dominated by the elastic tail. While RIXS measurements at the U  $N_{4,5}$  edges ( $4d \rightarrow 5f$ ) in the soft x-ray range have been successful for U oxide samples [28, 29], no intensity was detected for U intermetallic samples. This is likely due to the combination of weak absorption at the U  $N_{4,5}$  edges and broader signals in intermetallics. The strong U  $M_{4,5}$  ( $3d \rightarrow 5f$ ) transition, however, falls within the tender x-ray regime, where achieving high resolution is a significant challenge. Currently, only one spectrometer in the world provides sufficient resolution: the MPI IRIX spectrometer at beamline P01 at DESY/PETRA-III, which was upgraded for ruthenate research [30].

At IRIX, we performed valence band RIXS measurements at the U  $M_{4,5}$  edges with sufficient resolution, enabling the detection of  $ff$  excitations in intermetallic uranium compounds with an excellent signal-to-background ratio. These  $ff$  excitations serve as unique fingerprints of the *formal* U  $5f$  configuration, helping resolve disputes concerning the formal valence states and confirming the presence of local physics and strong correlations in these itinerant compounds. Additionally, the orientation dependence of the multipolar excitations in NIXS (and to some extent in RIXS) provides crucial information about

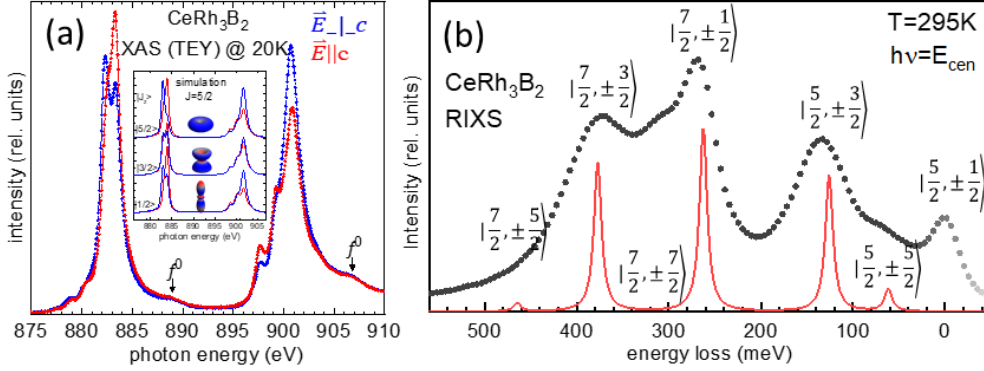


Fig. 1: RIXS: (a) XAS data of  $\text{CeRh}_2\text{B}_2$  for linear linear polarized light and simulation for pure  $|J = \frac{5}{2}, J_z\rangle$  states in inset in (a). RIXS data (black dots) of  $\text{CeRh}_2\text{B}_2$  at 295 K measured at resonance energy of the Ce  $M_5$  edge with full multiplet simulation assuming a  $|J = \frac{5}{2}, J_z = \pm \frac{1}{2}\rangle$  ground state (red line) (b).

orbital occupation.

PES, on the other hand, is sensitive to covalence. For rare earth compounds, the quantitative analysis of core-level PES data using configuration interaction-type calculations is relatively straightforward [31]. However, this approach is not feasible for U intermetallics, where hybridization is significantly stronger, leading to contributions from multiple  $5f^n$  configurations (e.g.  $n = 0$  to 5) to the non-integer valent ground state. In such cases, more sophisticated approaches are necessary. Specifically, a combination of valence band (VB) PES measurements with both soft and hard x-rays is employed to distinguish subshells. This enables the determination of reliable material-specific parameters for density-functional theory (DFT) combined with dynamical mean-field theory (DMFT) calculations. This integrated approach of PES and DFT + DMFT provides new, reliable quantitative insights into the number of electrons in the  $5f$  shell and their degree of covalence.

The report begins with the most significant results on Ce compounds, followed by the group's initial findings aimed at gaining a deeper understanding of the electronic structure of U intermetallic compounds.

### Orbital selective coupling in $\text{CeRh}_3\text{B}_2$ : Coexistence of high Curie and high Kondo temperatures [19]

The seemingly contradictory properties of strong intermediate valency with a high Kondo temperature ( $\approx 400$  K) and ferromagnetic order with an exceptionally high ordering temperature ( $T_C = 115$  K), coupled with a significantly reduced ordered magnetic moment in the so-called *giant crystal-field* compound  $\text{CeRh}_3\text{B}_2$  [32, 33], have been investigated using a combination of XAS, RIXS at the Ce  $M_{4,5}$ -edges, and *ab initio* DFT calculations.

The point symmetry of Ce in  $\text{CeRh}_2\text{B}_2$  is hexagonal, meaning the crystal-field ground state must be a pure  $J_z$

state. The linearly polarized XAS data in Figure 1a, as well as the RIXS data in Figure 1b, are best described by the expected ground state symmetry of  $|J = \frac{5}{2}, J_z = \pm \frac{1}{2}\rangle$ . However, in XAS, the experimental dichroism is smaller than the theoretical prediction, and the RIXS data show intensities corresponding to  $\Delta J_z > 1$  that are more pronounced in the experiment than anticipated from the calculations.

In combination with DFT, we find that the ground state must have multi-orbital character. The state  $|J = \frac{5}{2}, J_z = \pm \frac{5}{2}\rangle$  contributes to the ground state, despite being forbidden by symmetry: the Kondo effect effectively mixes the  $|J = \frac{5}{2}, J_z = \pm \frac{5}{2}\rangle$  state at  $\approx 60$  meV with the  $|J = \frac{5}{2}, J_z = \pm \frac{1}{2}\rangle$  at zero energy. This intermixing accounts for the experimental observations of reduced dichroism and enhanced transition intensities. Furthermore, the presence of two distinct active Ce  $4f$  orbitals, each selectively coupling to different bands in  $\text{CeRh}_3\text{B}_2$ , explains the unusual combination of properties. The inter-site hybridization of the  $|J = \frac{5}{2}, J_z = \pm \frac{1}{2}\rangle$  crystal-field state and Ce  $5d$  band, combined with the intra-site Ce  $4f$ - $5d$  exchange, creates the strong ferromagnetism. Meanwhile, the hybridization between the  $|J = \frac{5}{2}, J_z = \pm \frac{5}{2}\rangle$  and the B  $sp$  orbitals in the  $ab$ -plane contributes to the Kondo interaction, which leads to the moment reduction.

### Spectroscopic evidence of Kondo-induced quasiquartet in $\text{CeRh}_2\text{As}_2$ [20]

$\text{CeRh}_2\text{As}_2$  is a newly discovered multiphase superconductor [11], with indications for an additional itinerant multipolar ordered phase [34]. We conducted core-level PES using hard x-rays (HAXPES) to confirm the presence of the Kondo effect in  $\text{CeRh}_2\text{As}_2$ . Additionally, we performed XAS at the Ce  $M_{4,5}(3d \rightarrow 4f)$  edges with linear polarized light to investigate the ground state orbital occupation.

The satellites observed in the HAXPES and isotropic XAS data confirm the presence of Kondo hybridization in  $\text{CeRh}_2\text{As}_2$ . Our findings indicate that the ground state must possess a Kondo-induced multiorbital character, as the thermal occupation of states alone cannot reproduce the temperature ( $T$ ) dependence of the linear dichroism  $\text{LD}(T)$ . In contrast, assuming a finite occupation of excited states due to the Kondo effect at low  $T$  provides a good description of  $\text{LD}(T)$  and the associated entropy, which suggests a quasi-quartet ground state. Such a quasi-quartet ground state, in turn, may allow the formation of a multipolar ordered phase.

For our results on  $\text{CeRh}_2\text{As}_2$  see Status Report [section 1.3](#).

### Singlet magnetism in intermetallic $\text{UGa}_2$ unveiled by inelastic x-ray scattering [22]

$\text{UGa}_2$  is a ferromagnetic U intermetallic compound with U–U distances well above the Hill limit. In the search for multiplet excitations in U intermetallic compounds,  $\text{UGa}_2$  appears to be a promising candidate due to its high Curie temperature and large magnetic moment ( $T_C=116\text{ K}$ ,  $\mu_{\text{ord}} > 3\mu_B$ ), which suggest that the  $5f$  electrons are on the more localized side.

The RIXS spectra of  $\text{UGa}_2$  exhibit three multiplet excitations in addition to elastic scattering [see Figure 2a], on top of charge transfer scattering, which is observable over a larger energy range that is not shown here. The two panels below present multiplet calculations based on a  $5f^2$  (middle) and  $5f^3$  configuration (bottom). The reduction of the Hartree-Fock values for the  $3d$ – $5f$  and  $5f$ – $5f$  Coulomb repulsion and  $5f$  spin–orbit interaction to 60, 55 and 90%, respectively, yields a good agreement

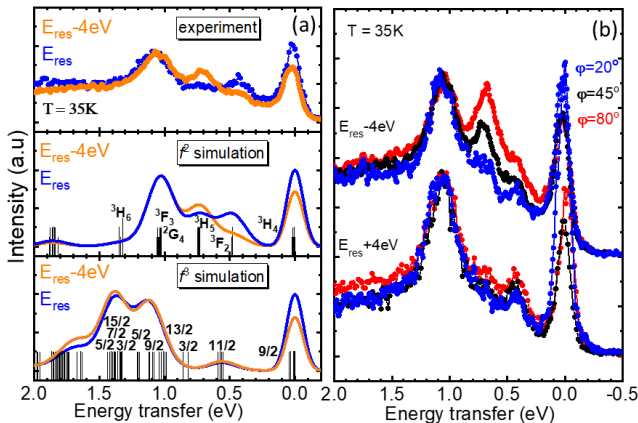


Fig. 2: (a) Top  $M_5$ -edge RIXS spectra of  $\text{UGa}_2$ , measured with incident energies at the  $M_5$  resonance (blue) and 4 eV below (orange), and full multiplet simulations based on the  $5f^2$  (middle) and  $5f^3$  configuration (bottom). (b) RIXS signal of  $\text{UGa}_2$  for different crystal orientations  $\phi$ , measured with two incident energies.

with the  $5f^2$  calculations. In contrast, no satisfactory accord could be achieved for the  $5f^3$ -based simulation. Therefore, the ground state must possess formal  $U 5f^2$  character and exhibit the symmetry of one of the states of the crystal-field split  $^3H_4$  multiplet in hexagonal point symmetry.

The energy resolution of the RIXS experiment is insufficient to resolve the crystal-field splittings, however, the impact of the anisotropic charge density is evident in the orientation dependence of the scattering signal when the sample is rotated (see Figure 2b). The NIXS data shown in Figure 3a, measured for momentum transfers parallel to the  $c$  and  $a$  axes, exhibit a strong direction dependence that aligns with a  $\Gamma_1$  singlet or  $\Gamma_6$  doublet state, as indicated by the full multiplet calculations in Figure 3b. However, for the ordered moment to lie in the hexagonal  $ab$  plane, the  $\Gamma_1$  singlet state must be the one lowest in energy. Therefore, the magnetism can be classified as either a singlet or induced-type of magnetism. Based on theoretical work by Thalmeier *et al.* [35, 36], we demonstrate that a  $\Gamma_1$ -singlet and  $\Gamma_6$ -doublet crystal-field state, split by energy  $\Delta$  and coupled by the effective exchange interaction  $I_2$ , can yield an in-plane ordered moment as high as  $3\mu_B$  (see Figure 3c).

Having established the  $M$ -edge RIXS technique, with the  $M_4$ -edge now also accessible, we are positioned to systematically investigate the *formal* valence states of U intermetallic compounds. For instance,  $\text{UTe}_2$  has been measured and exhibits the typical multiplet excitations of the  $U 5f^2$  configuration [24].

For results on  $\text{UGa}_2$  see Status Report [section 1.3](#).

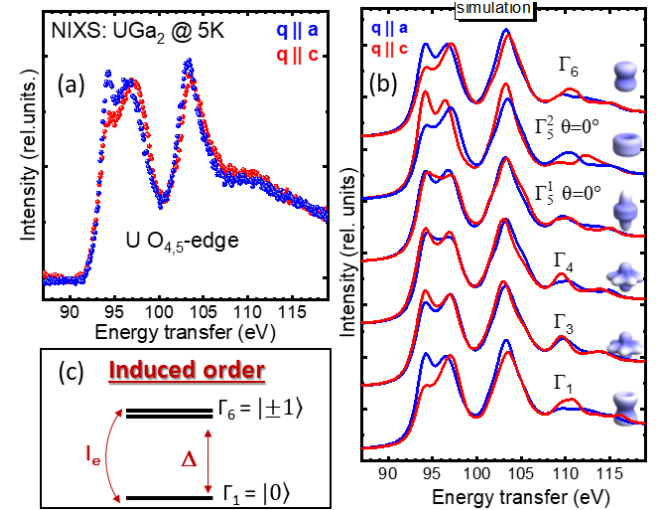


Fig. 3: (a) NIXS spectra of  $\text{UGa}_2$  for  $|\vec{q}| = 9.6 \text{ \AA}^{-1}$  for  $\vec{q} \parallel c$  and  $\vec{q} \parallel a$  with  $a$  and  $c$  hexagonal axis. (b) full multiplet simulation of NIXS spectra for six possible crystal-field states for  $U^{4+}$  in hexagonal point symmetry. (c) Induced order:  $\Gamma_1$  singlet states coupling by effective exchange  $I_e$  to  $\Gamma_6$  doublet, split by energy  $\Delta$ .

### Quantifying the U $5f$ covalence and degree of localization in U intermetallics [23]

We demonstrate the effectiveness of a combined photon-energy-dependent VB PES and DFT + DMFT study using two model materials:  $\text{UGa}_2$  and  $\text{UB}_2$ . The former is the aforementioned high  $T_C$  ferromagnet expected to be a more localized candidate, while the latter being a Pauli paramagnet with U–U distances well below the Hill limit, suggesting it represents the delocalized end of the localization–delocalization spectrum. Additionally,  $\text{UGa}_2$  exhibits multiplet excitations in the RIXS spectra (see above) and large satellites in the  $4f$  core-level PES, whereas  $\text{UB}_2$  neither shows multiplet excitations in RIXS nor satellites in the core-level spectra. Reliable material-specific values for the Hubbard  $U$ , Hund’s  $J$  and double counting correction  $\mu_{dc}$  were identified by reproducing the soft and hard x-ray VB spectra with the same set of parameters.

This study demonstrates that the  $5f^2$  configuration is the most prevalent in both compounds, with each exhibiting an average  $5f$  shell filling of  $\approx 2.2$ . However, for  $\text{UB}_2$ , the distribution of configurations contributing to the non-integer valent ground state is much broader and nearly statistically distributed. Furthermore, the time dependent charge correlation function is larger at  $t=0$  and decays significantly faster over time than that for  $\text{UGa}_2$ . This indicates that  $\text{UB}_2$  is indeed an itinerant, almost band-like material, whereas  $\text{UGa}_2$  is strongly correlated.

For our results on DFT+DMFT see Status Report [section 1.3](#).

### Fe substitution in $\text{URu}_2\text{Si}_2$ : Singlet magnetism in an extended Doniach phase diagram [21]

In this study we investigate the impact of substitution using Fe substituted  $\text{URu}_2\text{Si}_2$ .  $\text{URu}_2\text{Si}_2$  is a well studied heavy fermion U compound [5] that is famous for its hidden order state below 17 K. Upon substitution of Fe,  $\text{URu}_{2-x}\text{Fe}_x\text{Si}_2$  is driven into an antiferromagnetic ground state for  $0.05 < x$ , even though the end member  $\text{UFe}_2\text{Si}_2$  remains a Pauli paramagnet down to the lowest temperature. The antiferromagnetic state is suppressed above  $x \approx 1$ . The similarity of the  $(x, T)$  and  $(p, T)$  phase diagrams suggests that the formation of antiferromagnetic order is due to *chemical* pressure. However, this does not explain the suppression of antiferromagnetism in the higher doping regime.

In previous studies, we demonstrated with NIXS that  $\text{URu}_2\text{Si}_2$  and  $\text{UFe}_2\text{Si}_2$  share the same ground state symmetry [25, 26], which implies that core-level PES data can be compared in a meaningful manner and that the degree of (de)localization can be qualitatively

inferred from the strength of the satellites. We performed U  $4f$  core-level PES across the substitution series  $\text{URu}_{2-x}\text{Fe}_x\text{Si}_2$  for ten concentrations of Fe [see Figure 4] using the NSRRC-MPI TPS 45A Submicron soft x-ray beamline in Taiwan. We find that the spectral weight of the satellites behaves non-monotonically with Fe concentration  $x$ : it initially increases, then decreases again, and levels out at higher Fe concentrations. If only one mechanism were at play – namely chemical pressure as suggested by several studies – the observed increase followed by a decrease would imply that hidden order should reappear at the Fe concentration where satellite strengths are identical to  $\text{URu}_2\text{Si}_2$ . However, this has not been observed. Thus, two mechanism must be in effect upon substitution: 1) chemical pressure stabilizing the smaller ion, namely  $\text{U}^{4+}$  with two  $f$ -electrons, which favors a magnetic state; and 2) an increase in hybridization due to the growing partial density (pDOS) of transition metal  $d$  states close to the Fermi level, which favors the Pauli paramagnetic state. As a result, we propose an extended Doniach phase diagram, with the  $d$ -electron pDOS as a third axis.

In  $\text{URu}_{2-x}\text{Fe}_x\text{Si}_2$ , magnetic order must also be induced. We discuss how the antiferromagnetic state, with ordered moments aligned parallel to the tetragonal  $c$  axis, can be formed through the coupling of the two singlet states,  $\Gamma_1$  or  $\Gamma_2$ , that are lowest in energy according to our NIXS results [25, 26].

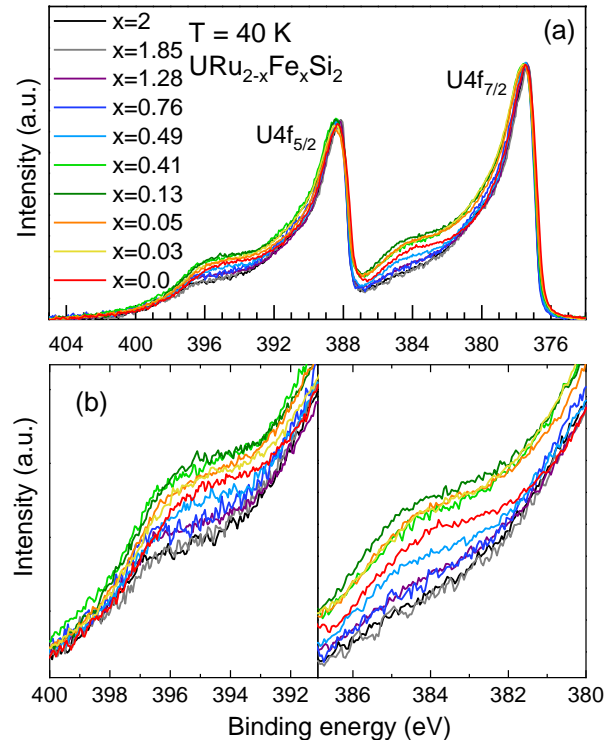


Fig. 4: (a) U  $4f$  core-level spectra of  $\text{URu}_{2-x}\text{Fe}_x\text{Si}_2$  for ten concentrations of Fe, (b) Satellites from (a) on an enlarged scale.

## External Cooperation Partners

Atsushi Hariki (Department of Physics and Electronics, Osaka Metropolitan University, Japan); Jan Kuneš (Department of Condensed Matter Physics, Masaryk University, Brno, Czechia); Philipp Hansmann (Department of Physics, Friedrich-Alexander Universität at Erlangen-Nürnberg, Germany); Maurits W. Haverkort (Institute for Theoretical Physics, Heidelberg University, Germany).

## References

- [1] P. Fulde, P. Thalmeier, and G. Zwicknagl, *Solid State Physics* vol. 60 (2006), *Strongly correlated electrons*
- [2] P. Coleman, *Handbook of Magn. and Adv. Magn. Mater.* vol. 1, John Wiley and Sons (2007), *Heavy Fermions: Electrons at the Edge of Magnetism*
- [3] *Superconducting phases of f-electron compounds*, C. Pfeiderer, *Rev. Mod. Phys.* **81** (2009) 1551, <https://dx.doi.org/10.1103/RevModPhys.81.1551>
- [4] *Electronic structure theory of the hidden-order material URu<sub>2</sub>Si<sub>2</sub>*, P. M. Oppeneer, J. Rusz, S. Elgazzar, M.-T. Suzuki, T. Durakiewicz, and J. A. Mydosh, *Phys. Rev. B* **82** (2010) 205103, <https://dx.doi.org/10.1103/PhysRevB.82.205103>
- [5] *Colloquium: Hidden order, superconductivity, and magnetism: The unsolved case of URu<sub>2</sub>Si<sub>2</sub>*, J. A. Mydosh, and P. M. Oppeneer, *Rev. Mod. Phys.* **83** (2011) 1301, <https://dx.doi.org/10.1103/RevModPhys.83.1301>
- [6] *The superconducting phases of UPt<sub>3</sub>*, R. Joynt, and L. Taillefer, *Rev. Mod. Phys.* **74** (2002) 235, <https://dx.doi.org/10.1103/RevModPhys.74.235>
- [7] *Nearly ferromagnetic spin-triplet superconductivity*, S. Ran, C. Eckberg, Q.-P. Ding, Y. Furukawa, T. Metz, S. R. Saha, I.-L. Liu, M. Zic, H. Kim, J. Paglione, and N. P. Butch, *Science* **365** (2019) 684, <https://dx.doi.org/10.1126/science.aav8645>
- [8] *Chiral superconductivity in heavy-fermion metal UTe<sub>2</sub>*, L. Jiao, S. Howard, S. Ran, Z. Wang, J. O. Rodriguez, M. Sgrist, Z. Wang, N. P. Butch, and V. Madhavan, *Nature* **579** (2020) 523 <https://dx.doi.org/10.1038/s41586-020-2122-2>
- [9] *Multicomponent superconducting order parameter in UTe<sub>2</sub>*, I. M. Hayes, D. S. Wei, T. Metz, J. Zhang, Y. S. Eo, S. Ran, S. R. Saha, J. Collini, N. P. Butch, D. F. Agterberg, A. Kapitulnik, and J. Paglione, *Science* **373** (2021) 797, <https://dx.doi.org/10.1126/science.abb0272>
- [10] *Topological superconductors: a review*, M. Sato, and Y. Ando, *Reports on Progress in Physics* **80** (2017) 076501, <https://dx.doi.org/10.1088/1361-6633/aa6ac7>
- [11] *Field-induced transition within the superconducting state of CeRh<sub>2</sub>As<sub>2</sub>*, S. Khim, J. F. Landaeta, J. Banda, N. Bannor, M. Brando, P. M. R. Brydon, D. Hafner, R. Kuechler, R. Cardoso-Gil, U. Stockert, A. P. Mackenzie, D. F. Agterberg, C. Geibel, and E. Hassinger, *Science* **373** (2021) 1012, <https://dx.doi.org/10.1126/science.abe7518>
- [12] F. de Groot, and A. Kotani, *Core Level Spectroscopy of Solis* vol. 6, CRC Press (2008), *Advances in Condensed Matter Science*
- [13] *Electronic Structure of Heavy Fermion Uranium Compounds Studied by Core-Level Photoelectron Spectroscopy*, S.-i. Fujimori, T. Ohkochi, I. Kawasaki, A. Yasui, Y. Takeda, T. Okane, Y. Saitoh, A. Fujimori, H. Yamagami, Y. Haga, E. Yamamoto, Y. Tokiwa, S. Ikeda, T. Sugai, H. Ohkuni, N. Kimura, and Y. Ōnuki, *Journal of the Physical Society of Japan* **81** (2012) 014703, <https://dx.doi.org/10.1143/JPSJ.81.014703>
- [14] *Core-Level Photoelectron Spectroscopy Study of UTe<sub>2</sub>*, S.-i. Fujimori, I. Kawasaki, Y. Takeda, H. Yamagami, A. Nakamura, Y. Homma, and D. Aoki, *J. Phys. Soc. Jpn.* **90** (2021) 015002, <https://dx.doi.org/10.7566/JPSJ.90.015002>
- [15]\* *Antiferromagnetic Correlations in Strongly Valence Fluctuating CeIrSn*, Y. Shimura, A. Wörl, M. Sundermann, S. Tsuda, D. T. Adroja, A. Bhattacharyya, A. M. Strydom, A. D. Hillier, F. L. Pratt, A. Gloskovskii, A. Severing, T. Onimaru, P. Gegenwart, and T. Takabatake, *Phys. Rev. Lett.* **126** (2021) 217202, <https://dx.doi.org/10.1103/PhysRevLett.126.217202>
- [16]\* *Quantitative investigation of the 4f occupation in the quasikagome Kondo lattice CeRh<sub>1-x</sub>Pd<sub>x</sub>Sn*, M. Sundermann, A. Marino, A. Gloskovskii, C. Yang, Y. Shimura, T. Takabatake, and A. Severing, *Phys. Rev. B* **104** (2021) 235150, <https://dx.doi.org/10.1103/PhysRevB.104.235150>
- [17]\* *Absence of magnetic field effect on the cerium valence in CeCu<sub>2</sub>Si<sub>2</sub> at its optimum superconducting critical temperature*, M. Barbier, M. Sundermann, A. Poux, A. Rogalev, D. Braithwaite, J.-P. Sanchez, and F. Wilhelm, *Phys. Rev. B* **104** (2021) 205136, <https://dx.doi.org/10.1103/PhysRevB.104.205136>
- [18]\* *Metamagnetism and crystal-field splitting in pseudo-hexagonal CeRh<sub>3</sub>Si<sub>2</sub>*, A. Amorese, D. Khalyavin, K. Kummer, N. B. Brookes, C. Ritter, O. Zaharko, C. B. Larsen, O. Pavlosiuk, A. P. Pikul, D. Kaczorowski, M. Gutmann, A. T. Boothroyd, A. Severing, and D. T. Adroja, *Phys. Rev. B* **105** (2022) 125119, <https://dx.doi.org/10.1103/PhysRevB.105.125119>
- [19]\* *Orbital selective coupling in CeRh<sub>3</sub>B<sub>2</sub>: Coexistence of high Curie and high Kondo temperatures*, A. Amorese, P. Hansmann, A. Marino, P. Körner, T. Willers, A. Walters, K.-J. Zhou, K. Kummer, N. B. Brookes, H.-J. Lin, C.-T. Chen, P. Lejay, M. W. Haverkort, L. H. Tjeng, and A. Severing, *Phys. Rev. B* **107** (2023) 115164, <https://dx.doi.org/10.1103/PhysRevB.107.115164>
- [20]\* *Spectroscopic Evidence of Kondo-Induced Quasi-quartet in CeRu<sub>2</sub>As<sub>2</sub>*, D. S. Christovam, M. Ferreira-Carvalho, A. Marino, M. Sundermann, D. Takegami, A. Melendez-Sans, K. D. Tsuei, Z. Hu, S. Rößler, M. Valvidares, M. W.

- Haverkort, Y. Liu, E. D. Bauer, L. H. Tjeng, G. Zwicky, and A. Severing, *Phys. Rev. Lett.* **132** (2024) 046401, <https://dx.doi.org/10.1103/PhysRevLett.132.046401>
- [21]\* *Fe substitution in URu<sub>2</sub>Si<sub>2</sub>: Singlet magnetism in an extended Doniach phase diagram*, A. Marino, D. S. Christovam, C.-F. Chang, J. Falke, C.-Y. Kuo, C.-N. Wu, M. Sundermann, A. Amorese, H. Gretarsson, E. Lee-Wong, C. M. Moir, Y. Deng, M. B. Maple, P. Thalmeier, L. H. Tjeng, and A. Severing, *Phys. Rev. B* **108** (2023) 085128, <https://dx.doi.org/10.1103/PhysRevB.108.085128>
- [22]\* *Singlet magnetism in intermetallic UGa<sub>2</sub> unveiled by inelastic x-ray scattering*, A. Marino, M. Sundermann, D. S. Christovam, A. Amorese, C.-F. Chang, P. Dolmantis, A. H. Said, H. Gretarsson, B. Keimer, M. W. Haverkort, A. V. Andreev, L. Havela, P. Thalmeier, L. H. Tjeng, and A. Severing, *Phys. Rev. B* **108** (2023) 045142, <https://dx.doi.org/10.1103/PhysRevB.108.045142>
- [23]\* *Quantifying the U 5f covalence and degree of localization in U intermetallics*, A. Marino, D. S. Christovam, D. Takegami, J. Falke, M. M. F. Carvalho, T. Okauchi, C.-F. Chang, S. G. Altendorf, A. Amorese, M. Sundermann, A. Gloskovskii, H. Gretarsson, B. Keimer, A. V. Andreev, L. Havela, A. Leithe-Jasper, A. Severing, J. Kuneš, L. H. Tjeng, and A. Hariki, *Phys. Rev. Res.* **6** (2024) 033068, <https://dx.doi.org/10.1103/PhysRevResearch.6.033068>
- [24]\* *Stabilization of U 5f<sup>2</sup> configuration in UTe<sub>2</sub> through U 6d dimers in the presence of Te<sub>2</sub> chains*, D. S. Christovam, M. Sundermann, A. Marino, D. Takegami, J. Falke, P. Dolmantis, M. Harder, H. Gretarsson, B. Keimer, A. Gloskovskii, M. W. Haverkort, I. Elfimov, G. Zwicky, A. V. Andreev, L. Havela, M. M. Bordelon, E. D. Bauer, P. F. S. Rosa, A. Severing, and L. H. Tjeng, *Phys. Rev. Res.* **6** (2024) 033299, <https://dx.doi.org/10.1103/PhysRevResearch.6.033299>
- [25] *Direct bulk-sensitive probe of 5f symmetry in URu<sub>2</sub>Si<sub>2</sub>*, M. Sundermann, M. W. Haverkort, S. Agrestini, A. Al-Zein, M. Moretti Sala, Y. Huang, M. Golden, A. de Visser, P. Thalmeier, L. H. Tjeng, and A. Severing, *Proc. Natl. Acad. Science. U.S.A.* **113** (2016) 13989, <https://dx.doi.org/10.1073/pnas.1612791113>
- [26] *From antiferromagnetic and hidden order to Pauli paramagnetism in UM<sub>2</sub>Si<sub>2</sub> compounds with 5f electron duality*, A. Amorese, M. Sundermann, B. Leedahl, A. Marino, D. Takegami, H. Gretarsson, A. Gloskovskii, C. Schlueter, M. W. Haverkort, Y. Huang, M. Szlawska, D. Kaczorowski, S. Ran, M. B. Maple, E. D. Bauer, A. Leithe-Jasper, P. Hansmann, P. Thalmeier, L. H. Tjeng, and A. Severing, *Proc. Natl. Acad. Sci. U.S.A.* **117** (2020) 30220, <https://dx.doi.org/10.1073/pnas.2005701117>
- [27] *Quanta for core level spectroscopy - excitons, resonances and band excitations in time and frequency domain*, M. W. Haverkort, *J. Phys. Conf. Ser.* **712** (2016) 012001, <https://dx.doi.org/10.1088/1742-6596/712/1/012001>
- [28] *Resonant inelastic x-ray spectroscopy on UO<sub>2</sub> as a test case for actinide materials*, G. H. Lander, M. Sundermann, R. Springell, A. C. Walters, A. Nag, M. Garcia-Fernandez, K. J. Zhou, G. van der Laan, and R. Caciuffo, *Journal of Physics: Condensed Matter* **33** (2020) 06LT01, <https://dx.doi.org/10.1088/1361-648X/abc4d2>
- [29]\* *Resonant inelastic x-ray scattering from U<sub>3</sub>O<sub>8</sub> and UN*, E. L. Bright, L. Xu, L. M. Harding, R. Springell, A. C. Walters, M. Sundermann, M. Garcia-Fernandez, S. Agrestini, R. Caciuffo, G. van der Laan, and G. H. Lander, *Journal of Physics: Condensed Matter* **35** (2023) 175501, <https://dx.doi.org/10.1088/1361-648X/acb8f4>
- [30] *IRIXS: a resonant inelastic X-ray scattering instrument dedicated to X-rays in the intermediate energy range*, H. Gretarsson, D. Ketenoglu, M. Harder, S. Mayer, F.-U. Dill, M. Spiwek, H. Schulte-Schrepping, M. Tischer, H.-C. Wille, B. Keimer, and H. Yavaş, *J. Synchrotron Rad.* **27** (2020) 538, <https://dx.doi.org/10.1107/S1600577519017119>
- [31] *Electron spectroscopies for Ce compounds in the impurity model*, O. Gunnarsson, and K. Schönhammer, *Phys. Rev. B* **28** (1983) 4315, <https://dx.doi.org/10.1103/PhysRevB.28.4315>
- [32] *Strong itinerant magnetism in ternary boride CeRh<sub>3</sub>B<sub>2</sub>*, S. K. Dhar, S. K. Malik, and R. Vijayaraghavan, *J. Phys. C: Solid State Physics* **14** (1981) L321, <https://dx.doi.org/10.1088/0022-3719/14/11/008>
- [33] *Superconductivity, magnetism and valence fluctuations in rare earth-transition metal borides*, M. Maple, S. Lambert, M. Torikachvili, K. Yang, J. Allen, B. Pate, and I. Lindau, *Journal of the Less Common Metals* **111** (1985) 239, [https://dx.doi.org/https://doi.org/10.1016/0022-5088\(85\)90192-4](https://dx.doi.org/https://doi.org/10.1016/0022-5088(85)90192-4)
- [34] *Possible Quadrupole Density Wave in the Superconducting Kondo Lattice CeRh<sub>2</sub>As<sub>2</sub>*, D. Hafner, P. Khanenko, E.-O. Eljaouhari, R. Kuchler, J. Banda, N. Bannor, T. Lühmann, J. F. Landaeta, S. Mishra, I. Sheikin, E. Hassinger, S. Khim, C. Geibel, G. Zwicky, and M. Brando, *Phys. Rev. X* **12** (2022) 011023, <https://dx.doi.org/10.1103/PhysRevX.12.011023>
- [35]\* *Induced order and collective excitations in three-singlet quantum magnets*, P. Thalmeier, *Phys. Rev. B* **103** (2021) 144435, <https://dx.doi.org/10.1103/PhysRevB.103.144435>
- [36]\* *Induced quantum magnetism in crystalline electric field singlet ground state models: Thermodynamics and excitations*, P. Thalmeier, and A. Akbari, *Phys. Rev. B* **109** (2024) 115110, <https://dx.doi.org/10.1103/PhysRevB.109.115110>

#andrea.severing@cpfs.mpg.de

##hao.tjeng@cpfs.mpg.de